X-RAY TOPOGRAPHY : PRINCIPLES

C. MALGRANGE

Laboratoire de Minéralogie-Cristallographie,
Université P. et M. Curie, 4 place Jussieu
75230 PARIS CEDEX 05 - FRANCE

1.- INTRODUCTION

Quite a lot of very good crystals are now available and their use is widening rapidly in modern technology.

Most physical properties depend on the defects of the crystal and interact with them. X-Ray topography methods (which are non destructive) give a two dimension projection image of the bulk defects of the crystal. The contrast on the topographs arises from the difference between the intensity diffracted by perfect and imperfect areas (section 3) and the propagation properties of X-Rays in slightly distorted crystals (section 4). Consequently,these methods give an image of the strain field in the crystal. The position of the defects in the crystal and their strain tensor can thus be determined in principle.

There are now quite a lot of different topographic methods with different and complementary fields of applications (for review see 1 to 6). A crude characterization of the defects (position for example) very helpful for a lot of applications (A. Mathiot conference) is quite easy but a careful interpretation leading to the value of the strain tensor around the defects is more difficult and requires a good knowledge of dynamical theory of diffraction in perfect and imperfect crystals.

Topographic methods can be divided in two main groups :

- reflexion methods : incident and diffracted X-Rays enter and leave the crystal surface at the same surface (fig. 1)
- transmission methods : X-Rays enter at a crystal surface and diffracted rays leave at the opposite surface.

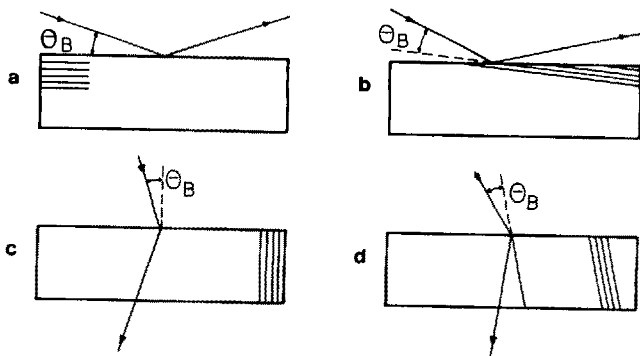

Fig. 1
Reflexion case : a) symmetric case, b) non symmetric case. Transmission case c) symmetric case, d)non symmetric case.

As a first approximation one can say that crystal thicknesses which can be studied by X-Ray topographic methods are such that the product of the linear absorption coefficient by the length of X-Ray path is of the order of 1. Bragg

angles being of the order of 10° this implies that crystal thicknesses can be greater in the case of transmission.

Typically, crystal thicknesses which can be studied by transmission vary from about 100 μm for high absorbing crystals to several millimeters for low absorbing crystals (containing light atoms). In the case of reflexion methods, the thicknesses which contribute to diffraction and thus which give images vary from about 1 to 20 μm.

One transmission method will be studied here in more detail : Lang method (7) , in order to show the basic principles of X-Ray topography. Then, synchrotron white radiation topography and double crystal topography will be described briefly.

2.- LANG METHOD

The incident beam coming from a point focus (∿ 100 μm x 100 μm) is collimated by a thin vertical slit (∿ 10 μm) S perpendicular to the plane of the figure 2. The crystal is adjusted so that the mean incident ray is at exact Bragg incidence for a characteristic radiation of the X-Ray tube and a given family of parallel (h,k,l) planes which we assume, for simplicity, to be perpendicular to the crystal surface. If the crystal is perfect, the divergence δ of the incident beam which contributes to the reflected beam is of the order of a few seconds. The corresponding X-Ray wave-fields propagate inside a triangle, the so-called

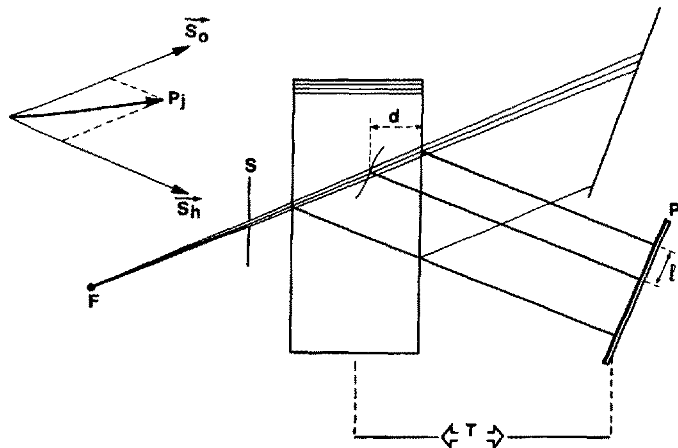

Fig. 2
Principle of Lang method

Borrmann fan giving rise to interference phenomena. Afterthis, the wave-fields split into two beams, one in the incident direction which we call the transmitted or refracted beam, the other in the reflected direction, the reflected beam. Due to interference phenomena the beams present fringes (Pendellösung or Katò fringes (8)) which are vertical lines if the crystal is parallel sided and hyperbola if it is a wedge shaped crystal.

Let us notice that the locus of the rays which are at exact Bragg incidence is a cone the apex of which is the focus, the axis being the normal to the reflected planes. The focus-crystal distance being of the order of 40 cm and the height of the crystal of the order of 1 cm, the rays at exact Bragg incidence form a sheet nearly perpendicular to the plane of the figure.

The divergence of the incident beam is of the order of 1 minute so that, for a perfect crystal,most of the incident beam is not reflected and propagates straightforward through the crystal, interacting with the crystal through photo-electric absorption only. If this part of the beam, called the direct beam, falls on a defect, a dislocation line for example, it can be diffracted by the distorted area surrounding the line and gives a black image on a photographic plate or film P perpendicular to the reflected beam. The position of the image in the beam is directly related to the depth of the defect which can then be measured ($l = 2\ d\ tg\theta$ in fig. 2). One thus obtains an image of the defects contained in a section of the crystal by the vertical sheet of incident X-Rays. This is the reason why Lang called this a "section topograph". If the crystal and the photographic plate are simultaneously translated along direction T one obtains an image which is a projection of the defects of the whole crystal. This image is called a traverse topograph. Of course the quantitative information on the depth of the defects in the crystal is lost with the translation and qualitative information only can be obtained by looking simultaneously at two "stereo images" ($h\ k\ l$ and $\bar{h}\ \bar{k}\ \bar{l}$ reflections).

The resolution of the method depends on two factors :

a) the broadening of the image due to experimental factors : in particular the focus size and the natural wavelength spread of the characteristic radiation which induce a divergence α of the beam diffracted by a point inside the crystal. The size s of the image is then equal to the product of this divergence α and the distance h crystal-film. With good experimental conditions s is of the order of 1 µm (details in ref. 4).

b) the intrinsic size of the image related to the strength of the strainfield around the defect as will be discussed just below.

3.- INTRINSIC WIDTH OF THE DIRECT IMAGE

The distorted area which contributes to the direct image corresponds to a local misorientation of the reflecting planes larger than something of the order of the angular width δ of the beam which can be reflected by a perfect crystal (2, 9). This region behaves as a small ideally imperfect crystal embedded in the perfect crystal and reflects X-Rays according to kinematical theory. The reflected intensity is thus proportionnal to the volume of the distorted area (Authier conference).

The size of this area depends on :

1) the value of δ which is

$$\delta \sim \frac{2|\chi_h|}{\sin 2\theta_B} \propto \frac{\lambda^2 F_h}{\sin 2\theta_B}$$

χ_h is the h Fourier coefficient of the electrical susceptibility.

δ depends on the wavelength and on the structure factor F_h of the considered reflection. Its order of magnitude is a second of arc.

The larger is δ,the smaller is the dimension of the zone which contributes to the direct image,so that the resolution, that is the possibility to separate two close defects, is higher for larger wavelengths and for stronger structure factors.
Table I give some orders of magnitude in the case of X-Rays, neutrons, and electrons. The scales are very similar for thermal neutrons and X-Rays. The high value of δ for electrons induces very narrow images leading to a higher resolution.

TABLE I

	λ	θ_B	F_h	δ	Λ
X-Rays	$\simeq$ 1 Å	$\simeq$ 10°	$\simeq 10^{-12}$ cm	$\simeq$ 1 sec	$\simeq$ 30 μm
Neutrons	$\simeq$ 1 Å	$\simeq$ 10°	$\simeq 10^{-12}$ cm	$\simeq$ 1 sec	$\simeq$ 30 μm
Electrons	$\simeq$ 0,05 Å	$\simeq$ 1°	$\simeq 10^{-8}$ cm	$\simeq$ 0,5°	$\simeq$ 300 Å

Orders of magnitude of characteristic parameters

λ : wave-length. θ_B : Bragg angle. F_h: structure factor. δ width of the reflexion profile. Λ : characteristic or Pendellösung or extinction length.
V : volume of the cell.

$$\Lambda \sim \frac{\pi V \cos\theta_B}{\lambda F_h} \qquad \delta \sim \frac{\lambda}{\Lambda \sin\theta_B}$$

2) on the choice of the reflecting planes which are more or less distorted. Figure 3 shows the example of an edge dislocation parallel to the surface of the crystal ; in a) the Burgers vector $\vec{b}$ is perpendicular to the reflecting planes which are the most distorted ones. The image is dark and wide. In b) the reflecting planes parallel

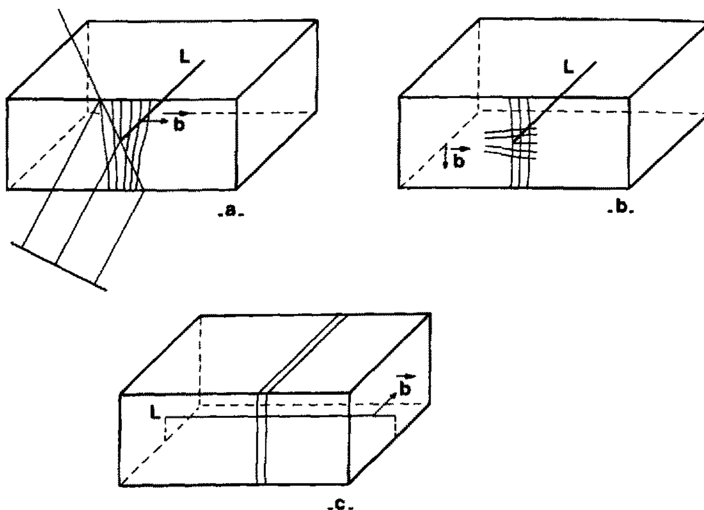

Fig. 3

to $\vec{b}$ and to the line are only slightly distorted. The image is very faint. In c) the reflecting planes perpendicular to L are not distorted. There is no image. This gives a means of determining the Burgers vector of a dislocation.

4.- PROPAGATION OF WAVEFIELDS IN DISTORTED AREAS

Let us now study the influence of defects on the part of the beam which is dynamically reflected and which spread over the Borrmann fan.

Let us consider a perfect crystal containing a slightly distorted area. By slightly distorted we mean that the variation of the departure from Bragg angle along a Pendellösung distance Λ is less than the width δ of the reflexion profile (Balibar conference). The Eikonal theory then holds and leads to a curvature of X-Rays paths (10 to 13) in distorted regions. Boundary conditions on the electric field at the entrance surface and considerations on the Poynting vector give the value of the intensity of the wavefield as a function of its direction. If we suppose, for simplicity, that absorption is zero, the intensity is constant along the path. Moreover, at the exit surface the splitting factor between reflected and refracted waves (intensity I_o and I_h respectively) is different from the corresponding one in the perfect crystal since Poynting vector $\vec{P}_j$ of wavefield j is given by :

$$\vec{P}_j \propto |D_o^j|^2 \ \vec{s}_o + |D_h^j|^2 \ \vec{s}_h \qquad \text{(fig. 2)}$$

Let us recall that $I_o \propto |D_o^j|^2$ and $I_h \propto |D_h^j|^2$.

This affects the repartition of the intensity along the basis of the Bormann fan (14). An example is shown in fig. 4 where distortions happen at the intersection of nearly screw dislocations with the surfaces of the crystal. The reflecting planes used for the topograph are radial planes for the dislocation and thus are not distorted, excepted near the surfaces where stress relaxation distortions are present (15).

In case of a value of the absorption small enough to give Pendellösung fringes, these fringes are distorted (16 to 20).

If the crystal is very distorted, geometrical optics do not apply anymore. Each wavefield induces a new wavefield (Balibar conference) which can interfere with ordinary wavefields leading to black and white fringes called, in the case of dislocations, intermediary images. Figure 5 shows these different types of images in the case of a dislocation. The X-Ray energy which would have been diffracted by the area surrounding the dislocation if it were perfect gives now curved wavefields and new wavefields which spread over a larger part of the Borrmann triangle basis. Therefore there is a lack of intensity along the shadow of the dislocation leading to a white image called the dynamic image.

A very important case of new created wavefields is obtained along a discontinuity in the crystal at the limit between two perfect zones (I and II).

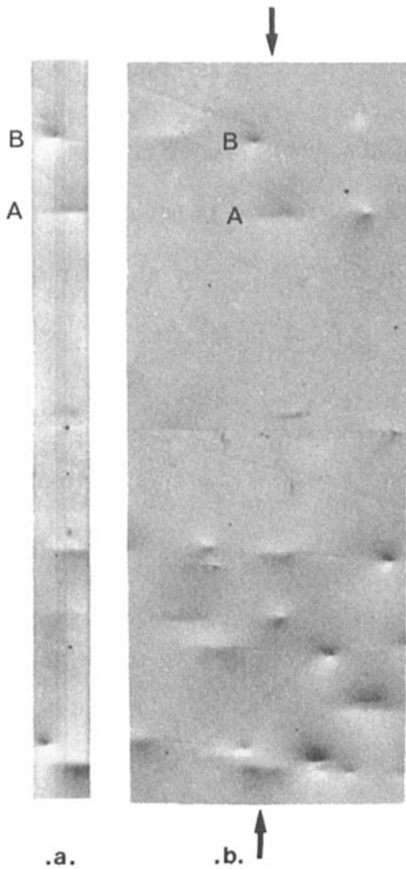

Fig. 4

a) Section topograph of a KDP crystal, (020), MoKα. A,B : images of stress relaxation distortions at the intersections of two different dislocations ; one cuts the entrance surface (A), the other the exit surface (B).
b) the corresponding traverse topograph.

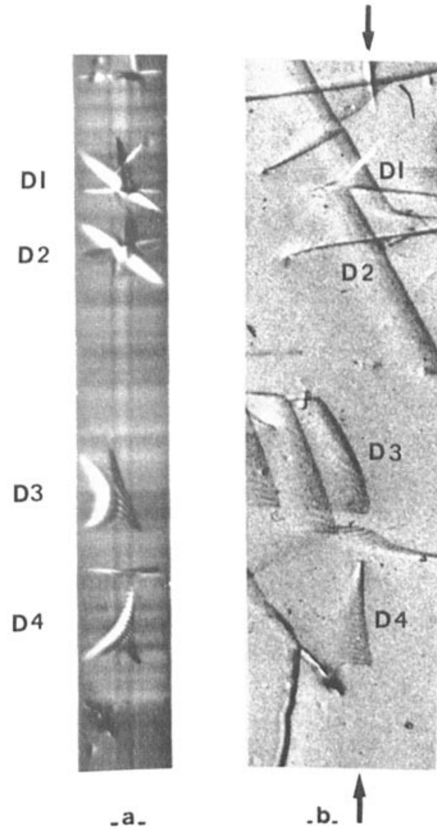

Fig. 5

a) Section topograph of a silicon crystal, (220), MoKα.
b) the corresponding traverse topograph. Note the blurring of the image as compared to the section.

Several cases may be considered and can occur simultaneously :

a) the two regions are translated with respect to one another through a translation which is not a translation of the lattice (stacking fault (21,22), antiphase boundary (23))...

b) the reciprocal lattice vector is different in the two regions (I and II are rotated with respect to one another (21) or/and have different lattice parameters. In each case characteristic fringes appear which have been experimentally observed and theoretically explained either using stationnary phase method (24) or by computer simulations (25, 26).

5.- SYNCHROTRON WHITE RADIATION TOPOGRAPHY (review articles 27, 28)

The source has very different characteristic features as compared to X-Ray tubes (Coïsson conference) :

- high flux of photons ;
- white radiation ;
- small emission divergence (order of 20 sec. for $\lambda \sim 1\text{Å}$ DCI ring in Orsay France) ;
- larger focus (order of 1,5mmx6mm) but located far (order of 20 m) from the sample.

Consequently,the divergence of the beam irradiating a point in the sample is of the same order as for classical X-Ray tube arrangements.

- due to the curvature of the electron orbit in the ring, the lateral extension of the beam is wide enough to cover the whole sample, every point of it being at Bragg incidence for slightly different wavelengths if the crystal is distorted. Consequently :

a) one obtains, without any translation, an image of the whole crystal even if it is made of several grains and several reflections alltogether.
b) the analysis of the contrast is different from classical Lang method (29, 30).
c) due to the high flux of photons, time exposures are reduced by a factor of the order of 50 allowing dynamic experiment (exposure time $\simeq$ 20 sec.)(31, 32).

6.- DOUBLE CRYSTAL TOPOGRAPHY

The principles of such arrangements are given in (33, 34, 35).

A first monochromator crystal is designed to obtain a monochromatic beam with an angular divergence $\Delta\theta$ smaller than the intrinsic width of the sample reflexion profile δ. Consequently there are no more"direct images" but a high sensitivity to small local distortions and the possibility to determine the sign of the distortion (34).

If the crystal is adjusted far from the maximum of the rocking curve, only those parts of the crystal which are very distorted (dislocation core for example) will contribute to the image leading to very thin images and thus a high resolution (37).

REFERENCES

[1] U. BONSE, M. HART, J.B. NEWKIRK : Advan. X-Ray Anal. 10, 9 (1967).

[2] A. AUTHIER : Advan. X-Ray Anal. 10, 9 (1967).

[3] A.R. LANG : Advan. X-Ray Anal. 10, 91 (1967).

[4] A.R. LANG in Modern Diffraction and Imaging Techniques in Material Science edited by S. Amelincks and al. North Holland p. 407 (1970).

[5] A. AUTHIER in Modern Diffraction... p. 481.

[6] A. AUTHIER in X-Ray Optics edited by H.J. Queisser, Springer-Verlag, p. 145 (1977).

[7] A.R. LANG : J. Appl. Phys. 29, 597, (1958).

[8] N. KATO : Acta Cryst. 14, 526 and 627 (1961)

[9] J. MILTAT, D.K. BOWEN : J. Appl. Cryst. 8, 657 (1975).

[10] P. PENNING, D. POLDER : Philips Res. Rept. 16, 419 (1961)

[11] P. PENNING : Thesis Delft (1966)

[12] N. KATO : J. Phys. Soc. Jap. 18, 1785 (1963).

[13] N. KATO : J. Phys. Soc. Jap. 19, 67, 971 (1964).

[14] C. MALGRANGE : International Summer School on X-Ray dynamical theory and topography. Limoges, France (1975).

[15] E. DUNIA, C. MALGRANGE, J.F. PETROFF : Phil. Mag. (1979), to be published.

[16] J.F. PETROFF, A. AUTHIER : Phys. Stät. Sol. 13, 373 (1966).

[17] N. KATO, Y. ANDO : J. Phys. Soc. Jap. 21, 964 (1966).

[18] Y.M. FISHMAN and V.G. LUTSAU : Phys. Stat. Sol. (a), 18, 443 (1973).

[19] N. KATO, J.R. PATEL : J. Appl. Phys. 44, 965, 971 (1973).

[20] Y. ANDO, J.R. PATEL, N. KATO : J. Appl. Phys. 44, 4405 (1973).

[21] A. AUTHIER, M. SAUVAGE : J. Physique 27, C3, 137 (1966).

[22] A. AUTHIER, J.R. PATEL : Phys. Stat. Sol. 27a, 213 (1975).

[23] B. CAPELLE, C. MALGRANGE : Phys. Stat. Sol. 20a, K5 (1973).

[24] A. AUTHIER : Phys. Stat. Sol. 27, 77 (1968).

[25] A. AUTHIER, Y. EPELBOIN : Phys. Stat. Sol. 41a, K9 (1977).

[26] T. KATAGAWA, H. ISHIKAWA , N. KATO : Acta Cryst. A31 , 246 (1975).

[27] B.K. TANNER : Progress Cryst. Growth 1, 23 (1977).

[28] M. SAUVAGE, J.F. PETROFF in "Synchrotron Radiation Research" edited by S. Doniach and H. Winick, Plenum Press, New-York (1979).

[29] B.K. TANNER, D. MIDGLEY, M. SAFA : J. Appl. Cryst. 10, 281 (1977).

[30] M. HART : J. Appl. Cryst. 8, 436 (1975).

[31] J. GASTALDI, C. JOURDAN : Phys. Stat. Sol. 49a, 529 (1978).

[32] J. MILTAT , D.K. BOWEN : J. Physique, 40, 389, (1979).

[33] U. BONSE, E. KLAPPER : Z. Naturforsch 13a, 348 (1958)

[34] U. BONSE : Z. Physik, 153, 278 (1958).

[35] H. HASHIZUME, K. KOHRA, T. YAMAGUCHI : Appl. Phys. Letters, 18, 213 (1971).

[36] U. BONSE : Z. Physik, 184, 71 (1965)

[37] J.F. PETROFF, M. SAUVAGE, P. RIGLET : Phil . Mag. To be submitted.